

Revisiting Mindlin's theory with regard to a gradient extended phase-field model for fracture

Resam Makvandi¹, Bilen Emek Abali², Sascha Eisentrager³, and Daniel Juhre^{1,*}

¹ Otto von Guericke University Magdeburg, Institute of Mechanics, Universittsplatz 2, 39106 Magdeburg, Germany.

² Technische Universitt Berlin, Institute of Mechanics, Einsteinufer 5, 10587 Berlin, Germany.

³ The University of New South Wales, School of Civil and Environmental Engineering, Sydney, NSW 2052, Australia.

The application of generalized continuum mechanics is rapidly increasing in different fields of science and engineering. In the literature, there are several theories extending the classical first-order continuum mechanics formulation to include size-effects [1]. One approach is the strain gradient theory with the intrinsic features of regularizing singular stress fields occurring, e.g., near crack tips. It is crucial to realize that using this theory, the strain energy density is still localized around the crack tip, but does not exhibit any signs of a singularity. Therefore, these models seem to be appropriate choices for studying cracks in mechanical problems. Over the past several years, the phase-field method has gathered considerable popularity in the computational mechanics community, in particular in the field of fracture mechanics [2]. Recently, the authors have shown that integrating the strain gradient theory into the phase-field fracture framework is likely to improve the quality of the final results due to the inherent non-singular nature of this theory [3]. In the present work, we will focus on a general formulation of the first strain gradient theory. To this end, the homogenization approach introduced in Ref. [4] is employed. It is based on a series of systematic finite element simulations using different loading cases to determine the equivalent material coefficients on the macro-scale (i.e., for a strain gradient elastic material) by taking the underlying micro-structure into account.

© 2021 The Authors *Proceedings in Applied Mathematics & Mechanics* published by Wiley-VCH GmbH

1 Introduction

Employing the phase-field method in fracture mechanics facilitates tracking crack interfaces by defining an additional degree of freedom, called the order-parameter, which distinguishes between damaged and intact material states. The total energy of fracture in the phase-field formulation usually includes the quadratic strain energy density function of the classical linear elasticity theory [2]. We have shown earlier that integrating the strain gradient theory in the phase-field modeling of fracture may improve the quality of the final results due to the inherent non-singular nature of this theory [3]. The current work aims to study the influence of using various strain gradient elasticity models on the performance of the enhanced phase-field fracture model.

2 Strain gradient extended phase-field fracture model

Considering only small deformations, we define the symmetric part of the displacement gradient, the linear strain tensor, $E_{ij} := \frac{1}{2}(u_{i,j} + u_{j,i})$, and its gradient, $H_{ijk} := E_{ij,k}$, where (and henceforth) we use Einstein's summation convention over the repeated indices; \mathbf{u} represents the displacement field, and the microscopic deformation gradient H_{ijk} is a third-order tensor that is symmetric with respect to its first two indices. Moreover, the stored elastic energy due to a specific displacement field is given as

$$\psi_{\text{el}} = \frac{1}{2} E_{ij} C_{ijkl} E_{kl} + \frac{1}{2} H_{ijk} D_{ijklmn} H_{lmn}. \quad (1)$$

While the first term in the right-hand side of Eq. (1) denotes the stored energy in classical continuum mechanics, the second term involves higher order derivatives of the displacement field, which corresponds to the so-called generalized continua (see also [5]). For an isotropic and centro-symmetric¹ material, the stiffness tensor,

$$C_{ijkl} = c_1 \delta_{ij} \delta_{kl} + c_2 (\delta_{ik} \delta_{jl} + \delta_{il} \delta_{jk}), \quad (2)$$

is given by Lamé constants, c_1 , c_2 , and the Kronecker delta. Moreover, the sixth-order material tensor,

$$\begin{aligned} D_{ijklmn} = & c_3 (\delta_{ij} \delta_{kl} \delta_{mn} + \delta_{in} \delta_{jk} \delta_{lm} + \delta_{ij} \delta_{km} \delta_{ln} + \delta_{ik} \delta_{jn} \delta_{lm}) + c_4 \delta_{ij} \delta_{kn} \delta_{ml} \\ & + c_5 (\delta_{ik} \delta_{jl} \delta_{mn} + \delta_{im} \delta_{jk} \delta_{ln} + \delta_{ik} \delta_{jm} \delta_{ln} + \delta_{il} \delta_{jk} \delta_{mn}) + c_6 (\delta_{il} \delta_{jm} \delta_{kn} + \delta_{im} \delta_{jl} \delta_{kn}) \\ & + c_7 (\delta_{il} \delta_{jn} \delta_{mk} + \delta_{im} \delta_{jn} \delta_{lk} + \delta_{in} \delta_{jl} \delta_{km} + \delta_{in} \delta_{jm} \delta_{kl}), \end{aligned} \quad (3)$$

* Corresponding author: e-mail daniel.juhre@ovgu.de

¹ In crystallography, centro-symmetry means indistinguishability of crystal data in a direction and the opposite direction [6].



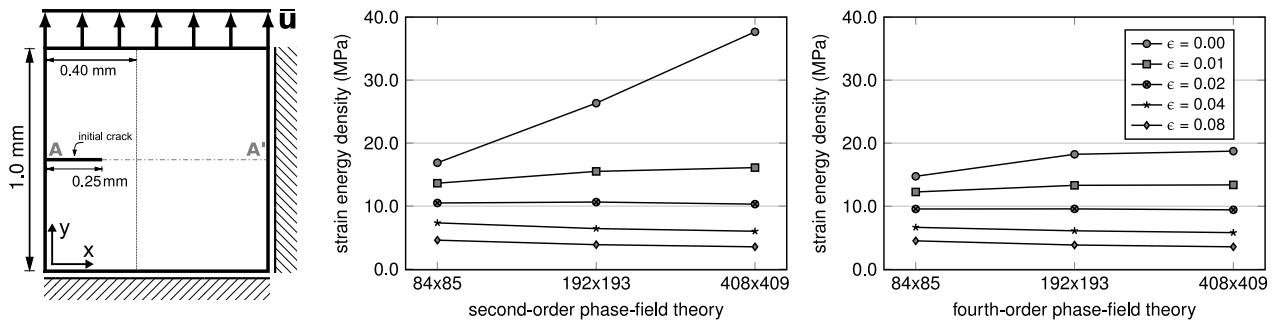


Fig. 1: Dimensions and boundary conditions of the problem ($\bar{u} = 0.1$ mm) (left). Comparison between the effective strain energy density ($s^2 \psi_{el}$) values on the crack front when the crack reaches $x = 0.40$ mm for the second-order (middle) and the fourth-order (right) phase-field models for different values of ϵ and three different mesh sizes ($\square \times \square$ denotes the number of control points in each parametric direction).

Table 1: Material properties used in lattice structures

Type	E (MPa)	ν
Matrix	118000	0.26
Inclusion	10^{-30}	10^{-30}

Table 2: Material properties used in the simulations

C_{1111} (MPa)	C_{1122} (MPa)	C_{1212} (MPa)			
26252	2228	618			
D_{111111} (N)	D_{111221} (N)	D_{111122} (N)	D_{221221} (N)	D_{221122} (N)	D_{122122} (N)
$5004 \epsilon^2$	$352 \epsilon^2$	$-274 \epsilon^2$	$5288 \epsilon^2$	$310 \epsilon^2$	$149 \epsilon^2$

introduces additional five material parameters, c_3 to c_7 , to the problem. In the present contribution, we use the method introduced in Ref. [4] to determine individual components of the stiffness and material tensors.

As for the total energy of the phase-field fracture part, we use two common formulations, that are referred to as the second-order and the fourth-order models, respectively

$$\bar{W}_{\text{frac}} = \int_{\Omega} \left[s^2 \psi_{el} + \mathcal{G}_c \left(\frac{(1-s)^2}{4\kappa} + \kappa |\nabla s|^2 \right) \right] dV - \int_{\Omega} \mathbf{b} \cdot \mathbf{u} dV, \quad (4)$$

$$\bar{W}_{\text{frac}} = \int_{\Omega} \left[s^2 \psi_{el} + \mathcal{G}_c \left(\frac{(1-s)^2}{4\kappa} + \frac{1}{2} \kappa |\nabla s|^2 + \frac{1}{4} \kappa^3 (\Delta s)^2 \right) \right] dV - \int_{\Omega} \mathbf{b} \cdot \mathbf{u} dV. \quad (5)$$

In Eqs. (4) and (5), s is the phase-field parameter ($s = 1$: intact material), \mathcal{G}_c represents the critical strain energy release rate, κ is the length-scale parameter for the crack, and \mathbf{b} denotes the vector of body forces. Calculating the first variations of Eqs. (4) and (5) gives us the variational formulations of the problem at hand for both the models. Due to the need for continuous derivatives of the shape functions between elements, we employ a NURBS-based isogeometric approach to solve the governing equations.

3 Numerical results

The material properties for the strain gradient part are provided in Tables 1 and 2. In Table 2, ϵ represents the so-called homothetic ratio [4]. Moreover, $\mathcal{G}_c = 2.0 \frac{\text{N}}{\text{mm}}$, $M = 2000.0 \frac{1}{\text{MPa} \cdot \text{s}}$ and $\kappa = 0.02$ mm. The results are presented in Fig. 1. The cut along path A-A' is identical to the expected crack propagation path. The case $\epsilon = 0.00$ recovers the classical continuum mechanics theory. While refining the mesh results in an increase in the value of the strain energy density for the classical theory. Increasing the homothetic ratio changes this behavior where the strain energy density is lower for the finer meshes. Hence, if the stress field is not singular near the crack tip, convergence of the results is observed. Moreover, the difference between the results of the second-order and fourth-order phase-field models is less significant for higher values of ϵ .

Acknowledgements Open access funding enabled and organized by Projekt DEAL.

References

- [1] P. Neff, I. D. Ghiba, A. Madeo, L. Placidi, and G. Rosi, *Continuum Mechanics and Thermodynamics* **26**(5), 639–681 (2014).
- [2] M. Ambati, T. Gerasimov, and L. de Lorenzis, *Computational Mechanics* **55**(2), 383–405 (2015).
- [3] R. Makvandi, S. Duczek, and D. Juhre, *Engineering Fracture Mechanics* **220**, 106648 (2019).
- [4] H. Yang, B. E. Abali, D. Timofeev, and W. H. Müller, *Continuum Mechanics and Thermodynamics* pp. 1–20 (2019).
- [5] R. D. Mindlin, *Archive for rational mechanics and analysis* **16** (1964), 51–78 (1964).
- [6] J. P. Mittal, I. Kaur, and R. C. Sharma, *Encyclopedia of Technical Education, Encyclopaedia of Technical Education* (Mittal Publications, 2015).